INDUSTRIAL HIGH-CURRENT ELECTRON LINACs*

A.S. Alimov[†], D.I. Ermakov[†], B.S. Ishkhanov[†], E.A. Knapp, V.I. Shvedunov[†], and W.P. Trower,
World Physics Technologies, Blacksburg VA 24060 USA

Abstract

We have designed a family of compact and modular **C**ontinuous **W**ave electron **LIN**ear **AC**celerators that produce 50 mA beams with energies from 0.6 to 10 MeV in increments of 600 keV for industrial, medical, and environmental irradiation applications. Here we report on the performance of our two-section 1.2 MeV/60 kW prototype.

1 INTRODUCTION

Table 1: CW LINAC parameters.

	One-Section	Two-Section
Beam energy	0.6 MeV	1.2 MeV
Beam current	0 to 50 mA	0 to 50 mA
Maximum beam power	30 kW	60 kW
Length	0.8 m	1.3 m
Gun/klystron high voltage	15 kV	15 kV
Plug power consumption	~75 kW	~150 kW
Electrical efficiency	~40%	~40%

Figure 1: Two-section (a) schematic and (b) test stand.
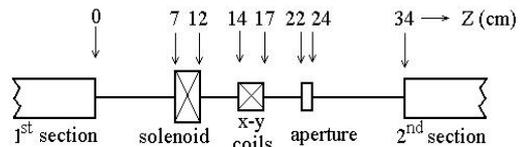
Figure 2: Beam line between the 1st and 2nd sections.

Our CW LINAC family will have ten accelerators each with beam currents of 50 mA, energies ranging from 0.6 to 6 MeV in increments of 600 keV, and corresponding beam power of 30 to 300 kW. We have now built prototypes of two of these accelerators whose parameters are listed in Table 1. Our one-section CW LINAC [1] provided a 600 keV/50 mA/30 kW exit beam. We report here results of the beam dynamics calculations, RF system design, and first experiments of our two-section 1.2MeV/50 mA/60 kW prototype seen in Fig. 1.

Our two-section CW LINAC consists of a 15 keV DC electron gun; 1st accelerating structure (14 cells with β from 0.237 to 0.888), which captures 42% of the gun electrons and accelerates the 50 mA beam to 600 keV; a beam line between 1st and 2nd structures; and the 2nd accelerating structure (9 cells, four with β = 0.914 and five with β = 0.945) which accelerates the 50 mA beam to 1.2 MeV.

2 TWO-SECTION BEAM DYNAMICS

In simulating the two-section accelerator beam dynamics, we used the measured 1st section diverging output beam parameters as input to the 2nd section: ~28 mm×mrad normalized emittance, ~3 mm radius, ~50° bunch length, ~51 mA average current, and 610 ± 20 keV energy. Thus we introduced between the sections a 0.06 T focusing solenoid, which provides transverse beam crossover at the 2nd structure center, as seen in Fig. 2

where the arrows longitudinally locate the element positions relative to the 1st structure exit. We also introduced coils to steer the beam and a cooled 1.2 cm diameter aperture that absorbs ~140 W of low-energy beam tail (~1.7 mA, ~80 keV) defocused by the solenoid.

At the 2nd section entrance, the beam, seen in Fig. 3, has a convergent ~3 mm radius and a longitudinal phase space that can be compressed by injecting the bunch with a phase advanced to that of the maximum RF acceleration phase. The maximum energy gain, Δ_{wmax}, is 693 keV, the power disappaited in the structure walls, P_{walls}, is 12.5 kW, and the injection phase, φ_{in}, is 60°, while the corresponding effective shunt impedance per unit length, R_{sh}, is 75 MΩ/m.
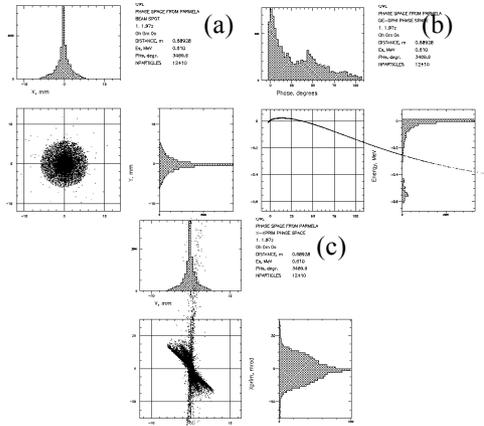
Figure 3: 2nd section entrance: (a) beam spot,
(b) longitudinal, and (c) transverse phase space.

Upon exiting the 2nd section, the beam, seen in Fig. 4 with parameters listed in Table 2, has lost ~0.5 kW uniformly over the nine section cells. The average electron loses ~83 keV.
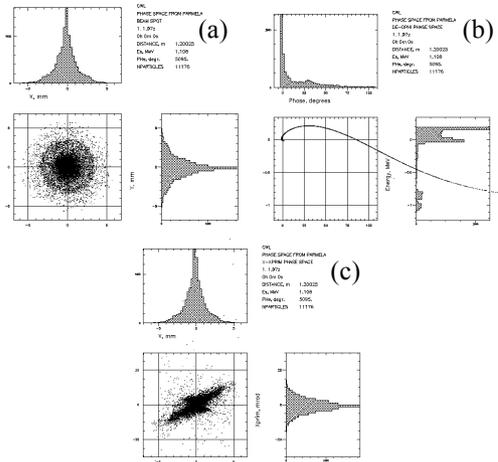
Figure 4: 2nd section exit: (a) beam spot,
(b) longitudinal, and (c) transverse phase space.

Table 2: Two-section CW LINAC exit beam.

I_{gun}	100 mA
I_{out}	49 mA
$\langle W_{beam}\rangle$	1.2 MeV
ΔW_{beam}	± 50 keV
$\Delta\varphi_{beam}$	~30°
Norm. $\langle\varepsilon_x\rangle$	11.2 mm×mrad
Norm. $\langle\varepsilon_y\rangle$	11.3 mm×mrad
Beam power	59 kW
Power losses	0.51 kW

3 RF SYSTEM

Our accelerator structures operate in a self-excited positive klystron-section feedback loop without a circulator. Thus they must be phased with each other since their frequencies are similar but unequal and their relative phase varies randomly. To phase the structures, we mix an external signal into the positive feedback loop between each structure and the klystron. We let the auto-oscillating 1st section provide the reference signal, eliminating a synchronizing oscillator [2]. Moreover, factors influencing self-excitation frequencies (e.g., cooling water temperature) act synchronously for the entire accelerator making its operation more stable.

The RF system, seen in Fig. 5, consists of a self-excitation feedback module for each structure and a module to mix the external signal into the feedback loop. Each feedback module low-power section has a RF probe in the structure feed cell, two directional couplers, a diode, a p-i-n attenuator, and a phase shifter. The external signal module has two 3 dB hybrids, a RF switch, a phase shifter, and a variable attenuator. The entire two structure low-power RF system includes attenuators (A_1-A_3), phase shifters (φ_1-φ_3), directional couplers (DC_1-DC_4), diodes (D_1-D_2), a RF switch (SW_1), and 3 dB hybrids (Hybrid$_1$-Hybrid$_2$).
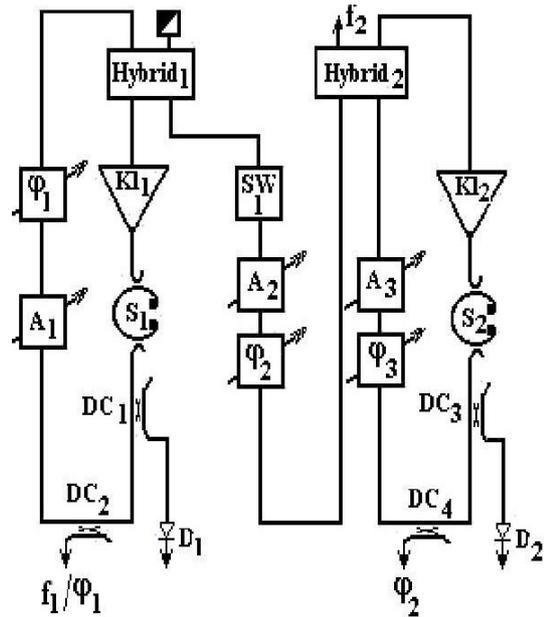
Figure 5: RF system block-diagram.

In each feedback loop, the structure probe signal passes through the p-i-n attenuator and the phase-shifter and then enters the klystron. The phase shifter chooses the self-excitation phase conditions while the feedback p-i-n attenuator regulates the klystron power and, consequently, the accelerating field amplitude that is controlled by the diode. In the 1st section feedback, the diode signal is also used by the amplitude stabilization system to control the p-i-n attenuator current. Thus the accelerating field

amplitude in the 1st section is stable to ~0.1%. The directional coupler signals are used to control the structure operational frequencies and the relative phase shift between them.

Part of the 1st section feedback signal (~0.5 W) via the 3 dB hybrid, RF switch, variable attenuator, and phase shifter enters the 3 dB hybrid in the 2nd feedback loop forming a synchronizing external signal for the 2nd section. With the RF switch (SW_1) turned off, each section auto-oscillates independently, but with the RF switch turned on, we observe synchronized two-section auto-oscillations. The external signal attenuator (A_2) regulates the synchronizing signal power while the phase shifter (φ_2) adjusts the phase shift between the structures.

4 BEAM EXPERIMENTS

We assembled our two-section CW LINAC and, using our existing industrial programmable logic controller based system, we measured the electron gun current (I_{gun}), the exit beam Faraday cup current (I_{out}), the power dissipated in each structure (P_{s1}, P_{s2}), which is the sum of the power dissipated in the structures walls (P_{walls1}, P_{walls2}) and the beam loss power (P_{loss1}, P_{loss2}), and the output beam power (P_{beam}), measured from the difference of the inlet and outlet cooling water temperatures at the Faraday cup. The principal measured parameters at various gun currents are listed in Table 3. Beam parameters derived from those measured are the beam energy ($W = P_{beam}/I_{out}$) and capture efficiency (I_{out}/I_{gun}).

Table 3: Two-section beam parameters.

I_{gun} (mA)	I_{out} (mA)	I_{out}/I_{gun} (%)	P_{beam} (kW)	W (MeV)
10	3.7	37	4.0	1.08
25	9.8	39	10.8	1.10
40	16.0	40	17.6	1.10
63	25.2	40	28.2	1.12
90	36.9	41	42.4	1.15
105	44.0	42	50.6	1.15

By adjusting the electron gun current, we varied the beam current from several mA to 44 mA. The beam energy increased with increasing beam loading until it reached 1.15 MeV at 44.0 mA (50.6 kW). To increase the beam current to its design value of 50 mA (60 kW), we must tune the 1st section klystron, whose maximum output power has been reduced from 50 kW to 45 kW during its 1.5 years in operation as a result of band-pass shifting. Figure 6 summarizes our beam tests and shows the 2nd section exit current dependence on gun current and the beam power dependence on 2nd section exit current.
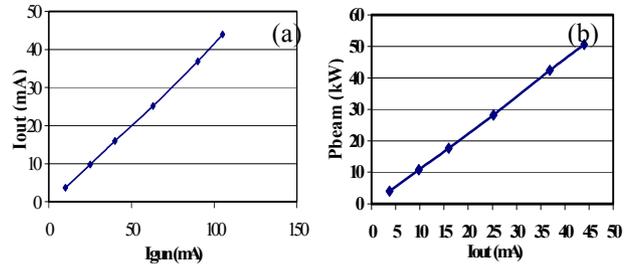
Figure 6: (a) I_{out} with I_{gun} and (b) P_{beam} with I_{out}.

5 CONCLUSION

We have constructed one- and two-section CW LINACs, the first in our family of industrial electron accelerators. In the two-section beam tests, we achieved a 1.15 MeV/44 mA/50.6 kW electron beam with a 105 mA gun current and a 42% capture efficiency. The two-section accelerator tests continue with full expectation that by adjusting the sub-systems parameters, we will obtain a 1.2 MeV/50 mA/60 kW exit beam and thus validate our design.

6 REFERENCES

[1] A.S. Alimov, D.I. Ermakov, B.S. Ishkhanov, E.A. Knapp, V.I. Shvedunov, and W.P. Trower, "Industrial High-Current Electron LINACs", in Proc. 2000 European Particle Accelerator Conf., J.L. Laclare, W. Mitaroff, Ch. Petit-Jean-Genaz, J. Poole, and M. Regler, eds. (World Scientific, Singapore, 2000) p. 803.

[2] A.S. Alimov, O.V. Chubarov, D.I. Ermakov, B.S. Ishkhanov, V.R. Yailijan, and V.I. Shvedunov, "Two methods of phasing the accelerator RF system with self-excitation", in Proc. 1996 European Particle Accelerator Conf., S. Maier, A. Pacheco, R. Pascual, Ch. Petit-Jean-Genaz and J. Pool, eds. (Institute of Physics, Bristol, 1996) p. 1908.